Lifetimes of Levels in $A=10$ Nuclei*

T. R. FISHER, S. S. HANNA, D. C. HEALEY, AND P. PAUL†
Department of Physics, Stanford University, Stanford, California 94305
(Received 6 June 1968)

The Doppler-shift attenuation method was used to obtain the following mean lifetimes (in psec) for the indicated nuclear levels: ^{10}C(3.36), $\tau=0.155\pm0.025$; ^{10}B(3.59), $\tau=0.150\pm0.015$; ^{10}Be(3.37), $\tau=0.189\pm0.020$; ^{10}B(2.15), $\tau=2.7_{-0.4}{}^{+0.5}$. A limit of $\tau<30$ fsec is obtained for ^{10}B(1.74), which is a factor of 8 greater than, and therefore consistent with, the lifetime computed from the analog β decay of ^{10}C. Transition strengths obtained from the ^{10}B(2.15) and ^{10}B(3.59) lifetimes are in good agreement with the effective-interaction calculations of Cohen and Kurath, as modified by Warburton *et al.* The ^{10}C(3.36) and ^{10}Be(3.37) states decay by analog $E2$ transitions: 2^+, $T=1\rightarrow 0^+$, $T=1$, with $T_z=\pm1$, whose strengths are well described by calculations of Kurath's for an effective charge $\epsilon_n=\epsilon_p=0.5$. An upper limit was obtained for the corresponding transition $5.17\rightarrow 1.74$ in ^{10}B($T_z=0$) which is consistent (factor of 4 greater) with the analog strengths observed in the $T_z=\pm1$ nuclei.

I. INTRODUCTION

ONE of the early successes of the intermediate-coupling model[1] was the correct prediction of the order of the low-lying levels of ^{10}B. With improved experimental technique it is now possible to test the theory more stringently by measuring the transition rates among the levels and comparing them with predicted values. The transitions involving the 0^+, $T=1$ level of ^{10}B can also be compared to the analog β transitions from ^{10}C. The extension of these measurements to the first excited levels in ^{10}Be and ^{10}C provides a comparison of radiation widths for $T=1$ analog levels. The energy level diagram showing the pertinent transitions is given in Fig. 1.

In a comprehensive study, Cohen and Kurath[2] have computed the transition rates in p-shell nuclei within a consistent theoretical framework based on nuclei in the complete p shell. On the experimental side, the advent of the lithium-drifted germanium detector with its greatly improved resolution has provided the impetus for undertaking new or improved measurements of the lifetimes of these states. In the present work, the Doppler-shift attenuation method has been applied to determine the lifetimes of the levels in ^{10}B at 1.74, 2.15, and 3.59 MeV,[3] and the levels in ^{10}Be and ^{10}C at 3.37 and 3.36 MeV, respectively (see Fig. 1). The goal was to obtain a consistent set of measurements within the same experimental framework. A search was also made[4] for the $5.17\rightarrow 1.74$ transition in ^{10}B, which is the isospin analog of the decays of the first excited states in ^{10}C and ^{10}Be. Measurements on some of these levels have been reported by other laboratories.[5,6]

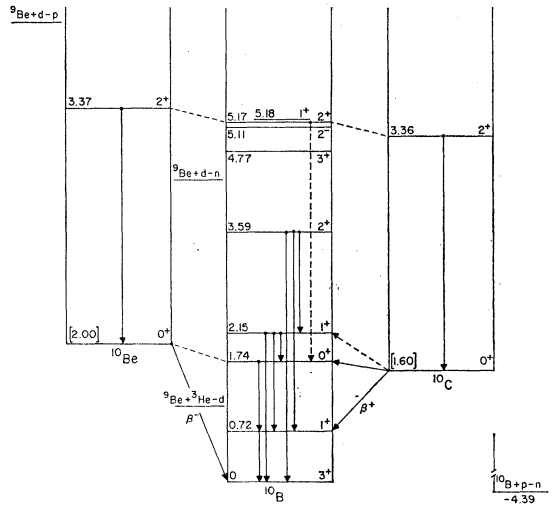

FIG. 1. Energy-level diagram of the $A=10$ system. Levels lying above the 2^+,$T=1$ levels are not depicted. Only those γ and β transitions pertinent to this experiment are shown. Transitions indicated by dashed lines have been sought but not observed.

The details of the method have been described earlier.[5,7] The main feature[8] of the method is the comparison of the Doppler shift of γ rays emitted by recoiling nuclei slowing down in a medium with that for recoils traveling in vacuum. The final results for the lifetimes are based on an analysis of the centroid displacements of the lines, but increased confidence in these results is derived by fitting the individual line shapes with computed curves.[7] The latter technique has been greatly refined in the present work.

II. CENTROID ANALYSIS

The principal features of the centroid analysis used in this work have been described previously.[7] In the present experiment, however, it was necessary to use care in treating the "nuclear" part of the slowing-down process and this treatment is presented here in detail.

* Supported in part by the National Science Foundation.
† Alfred P. Sloan Fellow. Present address: State University of New York at Stony Brook, N. Y.
[1] D. R. Inglis, Rev. Mod. Phys. **25**, 390 (1953).
[2] S. Cohen and D. Kurath, Nucl. Phys. **73**, 1 (1965).
[3] An early account of these measurements appears in T. R. Fisher, S. S. Hanna, and P. Paul, Phys. Rev. Letters **16**, 850 (1966).
[4] P. Paul, T. R. Fisher, and S. S. Hanna, Phys. Letters **16**, 850 (1966).
[5] E. K. Warburton, J. W. Olness, K. W. Jones, C. Chasman, R. A. Ristinen, and D. H. Wilkinson, Phys. Rev. **148**, 1072 (1966); E. K. Warburton, J. W. Olness, and A. R. Poletti, *ibid.* **160**, 938 (1967).
[6] D. J. Donahue, M. J. Wozniac, R. L. Hershberger, J. E. Cummings, and J. A. Lonergan, Phys. Rev. **165**, 107 (1968).
[7] P. Paul, J. B. Thomas, and S. S. Hanna, Phys. Rev. **147**, 774 (1966).
[8] R. W. Krone, A. Everett, and S. S. Hanna, Bull. Am. Phys. Soc. **1**, 329 (1956).

When a high-A material such as gold is used as the stopping medium, the effects of nuclear stopping and scattering may be so large that, for instance, the lifetime value of $^{10}C^*$ measured with Au is changed by 40% when the nuclear term is left out of the analysis. Range-energy data[9] are available for the stopping of light ions in medium and heavy materials, and these data provide the starting point for any realistic treatment of the nuclear stopping effect.

Two approaches to the description of the nuclear stopping have been taken. In the technique introduced by the Brookhaven group[5] the nuclear stopping effect is represented by the inclusion of a $1/v$ term in the energy-loss function. The mangitude of this term is determined by fitting available range-energy data, and the appropriate contribution to the centroid shift and spectral line shape may then be calculated.[5] (The nuclear contribution can also be inferred from line-shape fits directly.) The second approach is to use the theoretical derivation of Lindhard *et al.*[10] together with the scattering calculation of Blaugrund[11] to fit the range-energy data. An adjustable, multiplicative parameter f_n is introduced to take into account discrepancies between the results of theory and experimental range data. For the cases relevant to the present experiment this parameter was close to unity, indicating that the theory gave a good representation of the slowing-down process. The theoretical formalism may then be incorporated into a computer program[12] which computes the attenuation factor F_m as a function of the mean life τ. Experimentally, F_m is observed as the ratio of the mean (or centroid) Doppler shift for recoil into the medium to that for recoil into vacuum.

Although the two approaches should give equivalent results, the second approach is perferred here for the following reason. The Blaugrund calculation appears to have a sound theoretical basis, whereas the justification for the $1/v$ term is purely heuristic. Therefore, considerably more faith can be placed in extrapolation or interpolation procedures based on the former approach. Such procedures are usually necessary, since the available range-energy and energy-loss data are far from complete. However, the approach involving the $1/v$ term also has desirable features. It simplifies the analysis of the data if the line shape is to be fitted as described in the following section, whereas a similar analysis involving the Lindhard-Blaugrund calculation would be excessively complicated and time consuming.

[9] D. Powers and W. Whaling, Phys. Rev. **126**, 61 (1962); W. R. Phillips and F. H. Read, Proc. Phys. Soc. (London) **81**, 1 (1963); P. H. Barker and W. R. Phillips, *ibid.* **86**, 379 (1965); J. A. Panontin, L. L. Schwartz, A. F. Stehney, E. P. Steinberg, and L. Winsberg, Phys. Rev. **140**, A151 (1965).

[10] J. Lindhard, M. Scharff, and H. E. Schiøtt, Kgl. Danske Videnskab. Selskab, Mat.-Fys. Medd. **33**, No. 14 (1963).

[11] A. E. Blaugrund, Nucl. Phys. **88**, 501 (1966); A. E. Blaugrund, D. H. Youngblood, G. C. Morrison, and R. E. Segel, Phys. Rev. **158**, 893 (1967).

[12] J. B. Thomas, Ph.D. thesis, Stanford University (unpublished); and F. Riess, P. Paul, J. B. Thomas, and S. S. Hanna, following paper, Phys. Rev. **176**, 1140 (1968).

The centroid analyses reported in this paper utilize the Lindhard-Blaugrund expressions. The kinematics of the reaction and the finite thickness of the target are taken into account. Excellent agreement is found between results obtained with nickel and with gold as stopping media. In the former material the nuclear effect is small, while in the latter it is very large.

III. LINE-SHAPE ANALYSIS

It is a logical extension of the centroid analysis to obtain the lifetime by fitting the shape of the γ-ray line, since Ge(Li) detectors make possible the observation of detailed features of this shape. The shape-fitting technique affords significantly better precision in the analysis for very short lifetimes, and more generally the ability to obtain a good fit to the experimental line shape greatly increases the confidence in any lifteime measurement.

As a starting point of our line-shape analysis, the rate of energy loss for a recoil traveling in a medium is assumed to be given by[5]

$$-dE/dx=K_n(v_0/v_p)+K_e(v_p/v_0)-K_3(v_p/v_0)^3, \quad (1)$$

where v_p is the projected velocity and $v_0=c/137$. This equation is integrated in Appendix A to give a function $\exp[-t(E',E)/\tau]$, which represents the distribution in time of γ rays emitted with an energy E by a recoiling nucleus whose initial recoil velocity corresponded to a fully Doppler-shifted energy E'.

In general, the excited state of interest will be populated in a reaction involving emission of an associated particle. Then the energy distribution of the γ rays depends on the triple-correlation function $W(\theta_{\text{c.m.}},\theta_\gamma,\phi)$, which involves the angle of emission $\theta_{\text{c.m.}}$ of the recoil nucleus in the center-of-mass system relative to the beam axis, the emission angle θ_γ of the γ ray relative to the beam axis, and the dihedral angle ϕ between the two emission planes defined by the recoil, γ, and beam directions.

We now limit the discussion to the case where the γ rays are observed at $\theta=0°$ (or 180°) which can be treated without prior knowledge of the particle-particle-γ correlation of the reaction. The line shape for recoil into vacuum is then given by

$$P(E')dE'=W_0(\theta_{\text{c.m.}})d\Omega, \quad (2)$$

where $W_0(\theta_{\text{c.m.}})$ is simply the triple correlation function $W(\theta_{\text{c.m.}},\theta_\gamma,\phi)=W(\theta_{\text{c.m.}},0,0)$ for collinear directions of the first and third "particles."[13] The quantities E' and $\theta_{\text{c.m.}}$ are related by

$$E'=E_0[1+v_{\text{c.m.}}/c+v_r(\cos\theta_{\text{c.m.}})/c]. \quad (3)$$

The unshifted γ-ray energy is E_0, and $v_{\text{c.m.}}$ and v_r are the center-of-mass velocity and the recoil velocity in the center-of-mass system. The fit to the vacuum line shape in effect determines $W_0(\theta_{\text{c.m.}})$. Thus we see that the

[13] L. C. Biedenharn, G. B. Arfken, and M. E. Rose, Phys. Rev. **83**, 586 (1951).

analysis of vacuum line shapes can be used to measure correlation functions in nuclear reactions.[14]

The stopped line shape may now be written in the form

$$N(E)dE=\left[\int P(E')\left(\frac{\partial}{\partial E}\exp[-t(E,E')/\tau]+\delta(E)\exp[-t(0,E')/\tau]\right)dE'\right]dE. \quad (4)$$

The second term in the parentheses arises from the presence of recoil nuclei which have already stopped before decaying. The integral is taken over the range in E' for which $E'>E$. The method of evaluating Eq. (4) and fitting it to the "stopped" line shape is given in Appendix B.

The general procedure for extracting a nuclear lifetime by shape fitting is then as follows. The vacuum and stopped lines are observed at $\theta=0°$ and $\theta\lesssim180°$. The vacuum line shapes are fitted to determine $P(E')dE'$ and the folding function representing the detector resolution. The forward and backward vacuum runs are used to fix E_0. In fitting the stopped line shape, E_0 is fixed except for a possible gain shift correction given by an observed shift in a reference source line. The remaining parameters discussed in the Appendix are varied simultaneously to obtain the best fit.[15] In fitting all lines the analysis is modified to take into account the finite thickness of the target.

Since the line shapes cannot actually be obtained at $\theta=180°$ and sometimes not at $\theta=0°$ because of the presence of beam tubes, it is necessary to consider the effect of a noncollinear correlation. In this case the correlation is not uniquely determined by the vacuum line shapes, and for an exact treatment it would be necessary to know this correlation. In practice, this is not a serious difficulty for $\theta\leq30°$ or $\geq150°$ due to the fact that for the linear part of the energy-loss function the fit is independent of the correlation.[7] A more thorough discussion of this point is to be found in Ref. 12.

Modifications in the above procedure are desirable in some cases. If a reference line of nearly the same energy as that of the observed γ ray is available, the parameters of the folding function can be obtained by fitting this line. In some cases, enough angular correlation information is available for an independent determination of the distribution $P(E')dE'$. In the case of a long lifetime, it may be desirable to vary E_0 in the fitting procedure, whereas a more reliable result for a short lifetime may be obtained by fitting the difference between the vacuum and stopped line shapes.

IV. ENERGY-LOSS DATA

Although several stopping media were used in the course of this work, the new results reported here for states with lifetimes around $\tau\sim10^{-13}$ sec are based on the use of Au and Ni, for which energy-loss data exist in the literature.[16] For the long lifetime of the 2.15-MeV state of ^{10}B, the element Ca was used because of its low density. Since no data are available for Ca, its stopping power was interpolated from other data and also "measured" by observing the Doppler shifts produced by Ca for several "known" lifetimes[12] (see below).

TABLE I. Summary of stopping-power data used in this experiment. The K coefficients are in units of keV/(μg/cm^2) and α_e in 10^{-13} sec. For the target media B and Be it was really necessary to know only K_e. However, we have tabulated f_n for all cases to show that the required nuclear stopping is well represented by, and in no case exceeds the value given, by the theory. The ratio K_n/K_e is listed to emphasize the role played by nuclear stopping. The ways of determining these data are discussed in the text. The values of K_3 are only rough estimates since they are unimportant in this work.

Ion	Medium	α_e	K_e	K_n/K_e	K_3	f_n
^{10}Be	Au	3.9	0.30	0.45	0.006	1.0
	Ni	3.3	0.77	0.11	0.013	0.75
	Be	5.1	2.4			1.0
^{10}B	Au	3.2	0.37	0.50	0.007	1.0
	Ni	2.6	0.98	0.135	0.016	0.75
	Sc	5.1	1.8			0.75
	Ca[a]	8.1	1.8	0.10	0.023	0.75
	Al	4.5	1.85			1.0
	C	4.1	3.0			1.0
	B	2.9	3.1			1.0
	Be	3.7	3.3			1.0
^{10}C	Au	2.4	0.48	0.55	0.008	1.0
	B	2.2	4.0			1.0

[a] As determined from "known" lifetime measurements.

A summary of all energy-loss data used in the analysis is given in Table I. The values of K_e and K_3 (when needed) were used in both the centroid and line-shape fitting programs. These values were extracted from the energy-loss data as was done in Ref. 5. In the centroid analysis, the Lindhard-Blaugrund expression was used, as discussed in Sec. II, and the parameter[11] f_n was adjusted to fit the reported range-energy data[9] as illustrated by the example in Fig. 2. The case for C ions stopping in Al is "close" to that of B ions in Al used in one of our early measurements. It is seen that $f_n=1$ is fairly consistent with the data. Other examples of the determination of f_n are to be found in Ref. 12. Interpolation was used to obtain the values of f_n corresponding to the actual cases in Table I. In most instances this parameter was close to unity as can be seen from the table.

In the line-shape analysis, the $1/v$ term was used as discussed in Sec. III. The magnitude of the coefficient K_n which multiplies this term [see Eq. (1)] was chosen to produce a centroid shift identical to that resulting

[14] P. Paul, S. S. Hanna, and G. D. Sprouse, Bull. Am. Phys. Soc. **9**, 704 (1964); P. M. Cockburn, W. Stark, and R. W. Krone, *ibid.* **13**, 85 (1968).

[15] T. R. Fisher, in Proceedings of the Fall Decus Symposium, Anaheim, Calif., 1967 (unpublished).

[16] D. I. Porat and K. Ramavataram, Proc. Roy. Soc. (London) **A252**, 394 (1959); Proc. Phys. Soc. (London) **77**, 97 (1961); **78**, 1135 (1961); Y. A. Teplova, V. S. Nikolaev, I. S. Dmitriev, and L. N. Fateeva, Zh. Eksperim. i Teor. Fiz. **42**, 44 (1962) [English transl.: Soviet Phys.—JETP **15**, 31 (1962)]; J. H. Ormrod and H. E. Duckworth, Can. J. Phys. **41**, 1424 (1963); J. H. Ormrod, J. R. MacDonald, and H. E. Duckworth, *ibid.* **43**, 275 (1965); J. R. MacDonald, J. H. Ormrod, and H. E. Duckworth, Z. Naturforsch. **21a**, 130 (1966); B. Fastrup, P. Hvelplund, and C. A. Sautter, Kgl. Danske Videnskab. Selskab, Mat.-Fys. Medd. **35**, No. 10 (1966).

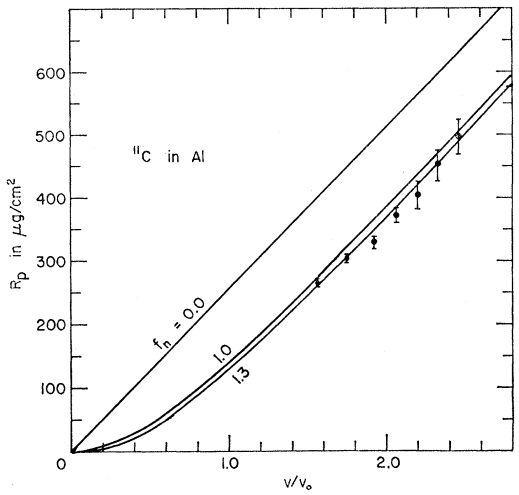

FIG. 2. Determination of f_n for ^{11}C ions stopping in Al. The range-energy data are those of Panontin *et al.* (Ref. 9). The adjustable parameter f_n multiplies the Lindhard-Blaugrund expression for the nuclear stopping term in the energy-loss formula.

from the Lindhard-Blaugrund expression in each case. No attempt was made to determine this coefficient directly from the range-energy data because of the interpolation problem mentioned in Sec. II.

V. EXPERIMENTAL ARRANGEMENT

For the measurements at bombarding energies below 3 MeV a Van de Graaff accelerator was used; above 3 MeV the results were obtained with a 9-MV tandem.

All the measurements were made with either ^{9}Be or ^{10}B targets. For the "stopped runs" these targets were prepared by evaporation onto backings of the desired stopping media. The Ca backings and some of the Au backings were also prepared by evaporation, the target layer being deposited following preparation of the backing. For the "vacuum runs" the targets were self-supporting foils prepared by evaporating the desired film onto a $BaCl_2$ substrate, floating the foils off on water, and picking them up on suitable frames.

The γ-ray spectra were obtained with a 25-cc coaxial Ge(Li) detector, which gave resolutions in the range 5–7 keV. The spectra were recorded in a 1024-channel analyzer, and suitable standard sources were used to monitor the gain of the system and the detector resolution. A standard run consisted of four measurements: two at an angle of 0° for recoil into vacuum and into a selected medium, and two at an angle of about 150° for the same recoil conditions.

VI. EXPERIMENTAL RESULTS

A. Levels ^{10}B*(3.59), ^{10}Be*(3.37), and ^{10}C*(3.36)

The lifetimes of these three states are approximately the same. The 3.37- and 3.36-MeV levels in ^{10}Be and ^{10}C are isospin analogs, and it will be seen that the 3.59-MeV level in ^{10}B provides a convenient experimental link between the lifetime measurements for these two closely related levels. Tables II–IV summarize the experimental results.

TABLE II. Summary of experimental results from the reactions ^{9}Be$(d,p)^{10}$B* and ^{9}Be$(d,n)^{10}$B* at $E_d=1.70$ MeV. Target thicknesses: 37 μm/cm^2 for Be foils, 37 μg/cm^2 for Be-Au targets, and 20 μg/cm^2 for Be-Ni targets. The values of F_m are the experimental numbers, and uncertainties quoted are statistical only.

Level	Peak (MeV)	Stopping medium	F_m	Av.
^{10}Be*(3.37)	2.35	Au	0.64	
			0.62	
			0.63	0.630±0.02
		Ni	0.65	
			0.66	0.655±0.02
^{10}B*(3.59)	1.85	Au	0.58	
			0.60	
			0.64	0.607±0.03
		Ni	0.69	
			0.68	0.685±0.03

TABLE III. Summary of experimental results from the reactions ^{10}B$(p,n)^{10}$C* and ^{10}B$(p,p')^{10}$B* at $E_p=9.5$ MeV. Target thicknesses: 40 μg/cm^2 for B foils and 100 μg/cm^2 for B-Au targets. Values of F_m are experimental numbers, and uncertainties quoted are statistical only.

Level	Peak (MeV)	Stopping Medium	F_m	Av.
^{10}C*(3.36)	2.34	Au	0.56	
			0.54	
			0.58	0.560±0.03
^{10}B*(3.59)	2.87	Au	0.66	
			0.58	
			0.67	0.637±0.04

TABLE IV. Summary of experimental results from the reaction ^{10}B$(p,p')^{10}$B* at $E_p=5.0$ MeV. Target thicknesses: 50 μg/cm^2 for both the B foil and the B-Au target. Values of F_m are experimental numbers, and uncertainties are statistical only.

Level	Peak (MeV)	Stopping medium	F_m
^{10}B*(3.59)	2.87	Au	0.60±0.03
	1.85	Au	0.60±0.04

1. Reactions ^{9}Be$(d,p)^{10}$Be(3.37) and ^{9}Be$(d,n)^{10}$B*(3.59)*

The deuteron bombarding energy was chosen as 1.70 MeV. This energy produces sufficient yield and avoids population of the next higher level in ^{10}Be at 5.96 MeV. A typical sequence of runs for the two-escape peak (2.35 MeV) of the 3.37-MeV transition in ^{10}Be is shown in Fig. 3. Interference from a background peak at 3.4 MeV prevented analysis of the full-energy peak (3.37 MeV). The spectra in Fig. 3 have been corrected for a contribution of about 12% from the one-escape peak (2.36 MeV) of the transition 3.59 → 0.72 MeV in ^{10}B. The ratio of intensities of the one-escape and two-escape peaks for the γ rays from a Th C'' source (2.615 MeV) was measured with the same 25-cc Ge(Li) detector. This ratio was used to determine the intensity of the contaminant one-escape peak from the intensity of the associated two-escape peak. The shape of the one-escape peak was assumed to be the same as that of the two-escape peak. Since the contaminant peak is associated with the ^{10}B level at 3.59 MeV, it has a Doppler shift similar to that of

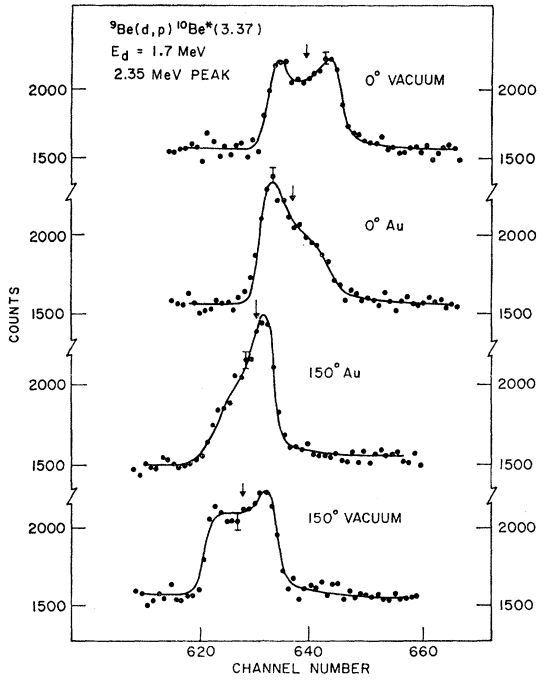

FIG. 3. Sequence of spectra for the two-escape peak of the 3.37-MeV γ ray from the reaction ^{9}Be$(d,p)^{10}$Be*(3.37). The curves are computer fits to the data. The arrows indicate the centroids of the lines.

the peak of interest and any uncertainty in the correction procedure is of negligible importance.

The solid curves in Fig. 3 and succeeding figures are the actual line-shape fits obtained with the general procedure outlined in Sec. III. As mentioned in Appendix B, for two-escape peaks it was found necessary to include an exponential tail on the high-energy side in the folding function to take into account Compton scattering of the escaping annihilation γ rays. However, the relative heights and widths of the Gaussian and exponential components were determined from the two-escape peak of a Th C'' source, so that only one free parameter, the width of the Gaussian component, remained to be determined from the vacuum line-shape fit. The apparent departure from front-back reflection symmetry in the peaks in Fig. 3 is mainly due to the exponential tail of the folding function. The structure in the "vacuum" peaks is due to forward and backward peaking in the angular distribution of the reaction cross section, as was verified by an independent measurement of this angular distribution. The arrows in Fig. 3 and succeeding figures indicate the centroids of the peaks.

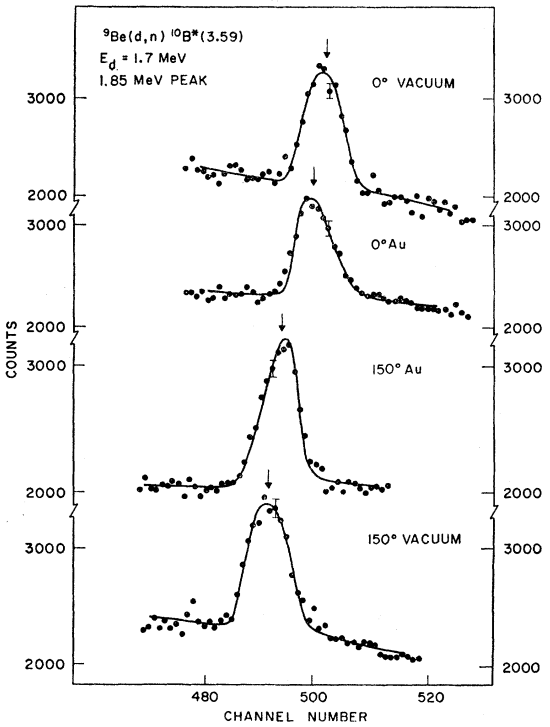

FIG. 4. Sequence of spectra for the two-escape peak of the 2.87-MeV γ ray from the reaction ^{9}Be$(d,n)^{10}$B*(3.59). The curves are computer fits to the data. The arrows indicate the centroids of the lines.

A sequence of runs for the two-escape peak (1.85 MeV) of the 3.59 → 0.72-MeV transition in ^{10}B is shown in Fig. 4. Again, the full-energy peaks could not be analyzed because of interference from other peaks. The experimental results are presented in Table II.

2. *Reactions $^{10}B(p,n)^{10}C^*(3.36)$ and $^{10}B(p,p')^{10}B^*(3.59)$ at $E_p=9.5$ MeV*

The proton bombarding energy was chosen above but as close to the ^{10}B$(p,n)^{10}$C* threshold as possible. Even so, it was necessary to take many precautions to reduce the background to a tolerable level. Targets used for the "stopped" measurements consisted of a 100-μg/cm^2 layer of boron backed by a 0.0001-cm layer of gold. The target chamber was plated internally with lead to decrease background from scattered protons. The beam, after passing through the target, excited into a lead-lined Faraday cup and stopped at a distance of several feet from the Ge(Li) detector.

A sequence of runs for the two-escape peak (2.34 MeV) of the 3.36-MeV transition in ^{10}C is shown in Fig. 5. The full-energy peak could not be analyzed due to interference from the two-escape peak (3.41 MeV) of the 4.43-MeV transition in ^{12}C. The spectra have been corrected for a 25% contribution from the one-escape peak (2.35 MeV) of the 3.59 → 0.72-MeV transition in ^{10}B by means of the procedure described above.

A sequence of runs for the full-energy peak (2.87 MeV) of the 3.59 → 0.72-MeV transition in ^{10}B is shown in Fig. 6. The experimental results are given in Table III.

3. *Reaction $^{10}B(p,p')^{10}B^*(3.59)$ at $E_p=5.0$ MeV*

At the reduced proton energy, background was not a serious problem and both the full-energy (2.87 MeV) and two-escape (1.85 MeV) peaks from the 3.59 → 0.72-MeV transition in ^{10}B could be analyzed. A sequence of

runs for the full-energy peak is illustrated in Fig. 7, and the results are presented in Table IV.

B. Level $^{10}B^*(2.15)$

This level provides a good illustration of the application of the Doppler-shift technique to the measurement of a long lifetime. For lifetimes of this magnitude (10^{-11} to 10^{-12} sec) a slow stopping medium is indicated. The best choice available appears to be calcium since lithium and sodium, although ideal in stopping power, are extremely reactive and usually create background problems. The evaporation of thick calcium layers is routine, and when the evaporated layer is protected by a thin layer of a nonreactive material it may be exposed to air for short periods of time without significant oxidation.

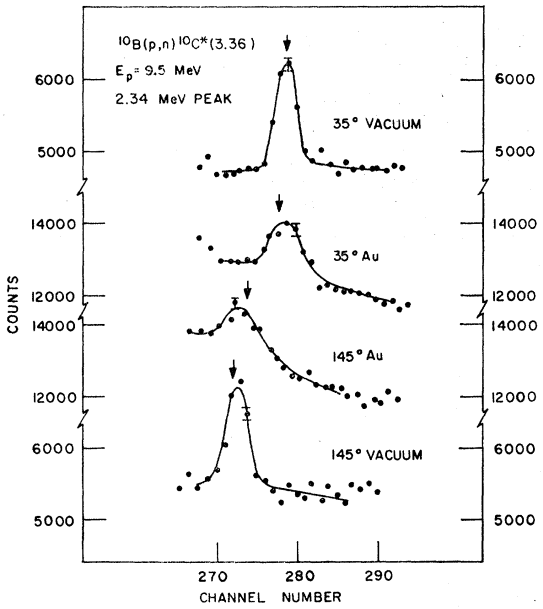

FIG. 5. Sequence of spectra for the two-escape peak of the 3.36-MeV γ ray from the reaction $^{10}B(p,n)^{10}C^*(3.36)$. The curves are computer fits to the data. The arrows indicate the centroids of the lines.

Unfortunately, no dE/dx curves for calcium have been measured, and the stopping-power data for nearby elements are scarce. The stopping parameters may be obtained by interpolation between fairly distant elements, but this is an uncertain procedure. In an attempt to obtain reliable values of K_e for light ions in calcium, the lifetimes of the first excited states of ^{7}Li and ^{7}Be as well as the 3.37- and 3.59-MeV levels of ^{10}Be and ^{10}B were measured using calcium as a stopping medium. The lifetimes were assumed known,[7] and values of K_e for lithium, beryllium, and boron ions in calcium were extracted from the measurements. The results were systematically about 20% higher than the interpolated values. An estimate of the possible oxygen contamination in the calcium layers based on density measurements gave an upper limit of 10%, insufficient to explain the discrepancy. However, the experimental

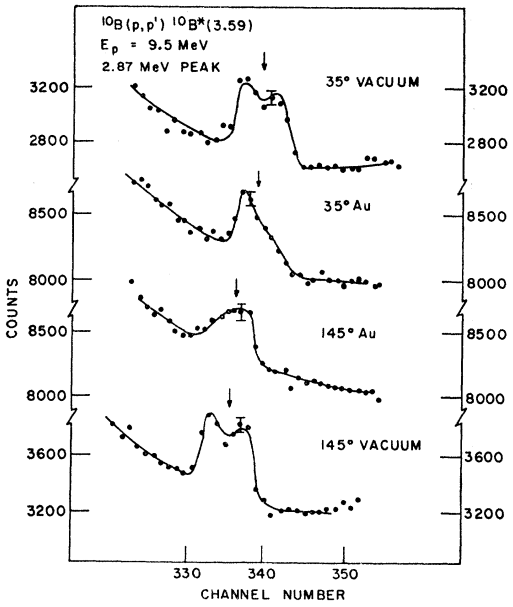

FIG. 6. Sequence of spectra for the full-energy peak of the 2.87-MeV γ ray from the reaction $^{10}B(p,p')^{10}B^*(3.59)$. The curves are computer fits to the data. The arrows indicate the centroids of the lines.

results present a consistent picture, and the "experimental" rather than the interpolated value of K_e for boron ions in calcium is given in Table I and used in this paper.

1. *Reaction $^{10}B(p,p')^{10}B^*(2.15)$ at $E_p=3.9$ MeV*

The 1.43-MeV γ ray from the transition $2.15 \rightarrow 0.72$ MeV in ^{10}B was observed at a proton bombarding energy chosen to avoid population of the 3.59-MeV level in ^{10}B, since the decay of this level to the 2.15-MeV

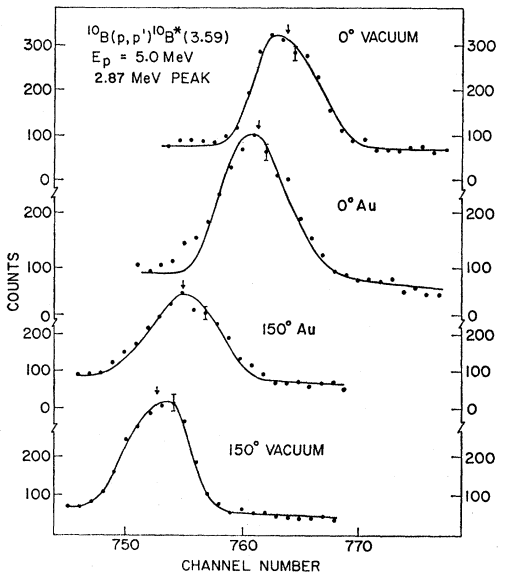

FIG. 7. Sequence of spectra for the full-energy peak of the 2.87-MeV γ ray from the reaction $^{10}B(p,p')^{10}B^*(3.59)$ at lower bombarding energy. The curves are computer fits to the data. The arrows indicate the centroids of the lines.

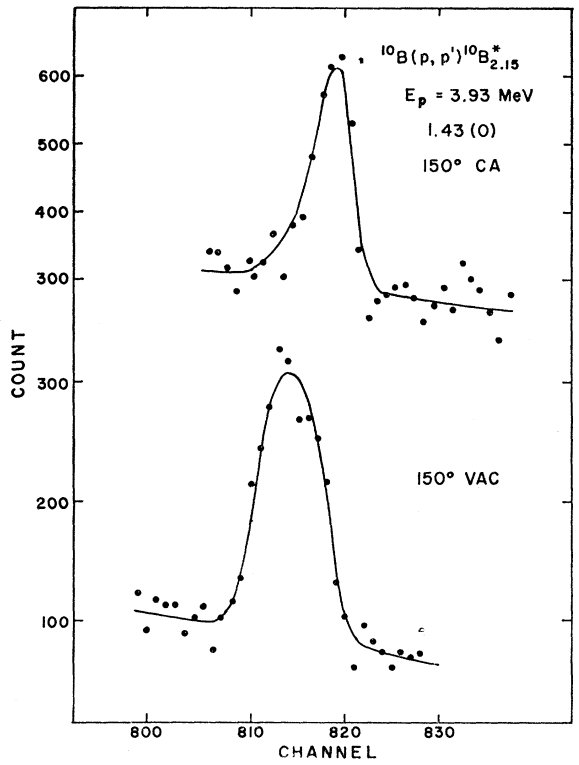

FIG. 8. Spectra at the backward angle for the full-energy peak of the 1.43-MeV γ ray from the reaction $^{10}B(p,p')^{10}B^*(2.15)$. The curves are computer fits to the data.

level produces a degenerate (in energy) 1.43-MeV γ ray. Measurements at the backward angle are illustrated in Fig. 8, and the experimental results are presented in Table V.

2. *Reaction $^9Be(^3He,d)^{10}B^*(2.15)$ at $E_p=2.8$ MeV*

A sequence of runs for the 0.41-MeV γ ray from the transition 2.15 → 1.74 MeV in ^{10}B is illustrated in Fig. 9. The 1.43-MeV line was not analyzed due to the degeneracy problem mentioned just above. Results of the measurements are presented in Table V.

3. *Reanalysis of Previous Measurements*

Our previous results for the 2.15-MeV level,[3] in which a variety of stopping media were used, were reanalyzed with newer energy-loss data[16] and the Lindhard-Blaugrund term. The new values of K_e are listed in Table I. The new results,[17] which agree with the present results with calcium, are listed in Table VI.

TABLE V. Summary of experimental results on the $^{10}B^*(2.15)$ level. Target thicknesses: 37 $\mu g/cm^2$ for Be foil, 38 $\mu g/cm^2$ for B foil, 37 $\mu g/cm^2$ for Be-Ca target, and 65 $\mu g/cm^2$ for B-Ca target. Values of F_m are experimental numbers, and uncertainties are statistical only.

Level	Reaction	Peak (MeV)	Stopping medium	F_m	Av.
$^{10}B^*(2.15)$	$^9Be(^3He,d)^{10}B^*$	0.41	Ca	0.158	
				0.228	
				0.192	0.193±0.034
	$^{10}B(p,p')^{10}B^*$	1.43	Ca	0.212	0.212±0.045

C. Level $^{10}B^*(1.74)$

The attempt to measure this very fast lifetime presents special problems. The only reaction available which is suitable for the present technique is $^9Be(^3He,d)^{10}B^*(1.74)$. In this reaction, the 1.74-MeV level is fed by the long-lived level at 2.15 MeV as well as being directly populated. At $E_{^3He}=2.8$ MeV, where a reasonably good yield is obtained for the reaction, the feeding is about 25% and uncertainties in its exact magnitude become serious. At 2.0 MeV, the feeding is only about 6%, but the low yield from the reaction makes it difficult to achieve good statistical precision. In addition, one faces the usual problem of minimizing the effect of target thickness.

Previously, we have quoted the limit $\tau<3\times10^{-14}$ sec for this lifetime.[3] Since then, more data have been amassed in an unsuccessful attempt to improve upon this limit significantly. The recent measurements were made at a bombarding energy of 2.0 MeV using targets consisting of 8 $\mu g/cm^2$ of Be on Au and a Be-Ca-Au sandwich: 8 $\mu g/cm^2$ of Be evaporated onto a 0.00005-cm Ca layer with a gold backing. With these targets the "fast" (i.e., directly populated) component decays in Au and in Ca, respectively, whereas the

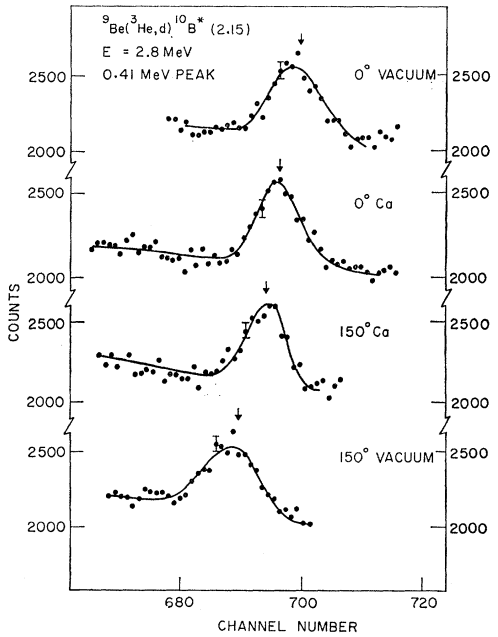

FIG. 9. Sequence of spectra for the 0.41-MeV γ ray from the reaction $^9Be(^3He,d)^{10}B^*(2.15)$. The curves are computer fits to the data. The arrows indicate the centroids of the lines.

[17] The use of the new values of K_e produces the greatest change in the results. The old values were based partly on the energy-loss measurement of Teplova *et al.* (Ref. 16), which were in disagreement with those of Porat and Ramavataram (Ref. 16) for low-Z media. The other references cited in Ref. 16 support the results of Porat and Ramavataram and lead to the new values obtained here.

"slow" (fed from the 2.15-MeV state) component in both cases decays predominantly in Au. Under these conditions the lifetime can be determined from a comparison of the spectra obtained with the two targets and the uncertainty in the amount of feeding from the 2.15-MeV level is of negligible importance. The composition of the targets was checked by observing the shifts of the 4.43-MeV γ ray from the reaction ^{9}Be(^{4}He,n)^{12}C(4.43), for which the lifetime is well known.[12]

The difference between the normalized spectra obtained with the two targets was analyzed using the line-shape technique, and a typical result is illustrated in Fig. 10. The minimum χ^2 in Fig. 10 is obtained for $\tau=1.0\times10^{-14}$ sec, but $\tau=0$ is not excluded. We choose to keep the limit $\tau<3\times10^{-14}$ sec quoted previously,[3] noting that the measurement in Fig. 10 allows only a 10% probability for τ to exceed this limit. A significant reduction of this limit does not appear feasible using the present technique.

D. Summary of Results

A summary of the results of the centroid and line-shape analyses for all lifetimes is given in Table VI. In all cases, the two techniques of analysis give results which are consistent within the experimental uncertainties. The final values adopted for the lifetimes are based on the centroid analysis since it is felt that this technique of analysis handles more correctly the nuclear stopping effect. However, the importance of consistency between the two techniques should be emphasized. In all cases, the line-shape analysis has proved invaluable to a complete understanding of the experimental data. In addition to statistical uncertainties, the final results quoted in Table VI include a 10% uncertainty in the values of K_e and a 5% uncertainty to account for possible error in the treatment of nuclear stopping effects.

TABLE VI. Summary of lifetime results. The final values adopted for the mean life τ are listed in the last column and are taken from the centroid analysis. The lifetimes are in units of 10^{-13} sec.

Level	Reaction	Stopping medium	τ (centroid)	τ (shape)	τ
^{10}Be*(3.37)	^{9}Be(d,p)^{10}Be*	Ni	1.90	1.90	
		Au	1.87	1.79	1.89±0.20
^{10}B*(3.59)	^{10}B(p,p')^{10}B* (E_p=5.0 MeV)	Au	1.48	1.42	
	^{10}B(p,p')^{10}B* (E_p=9.5 MeV)	Au	1.65	1.30	
	^{9}Be(d,n)^{10}B*	Ni	1.40	1.60	
		Au	1.60	1.54	1.50±0.15
^{10}C*(3.36)	^{10}B(p,n)^{10}C*	Au	1.55	1.49	1.55±0.25
^{10}B*(2.15)	^{9}Be(^{3}He,d)^{10}B*	Ca	28	26	
		Be	30[a]		
		Al	33[a]		
		Sc	36[a]		
		Ni	30[a]		
	^{9}Be(d,n)^{10}B*	Be	28[a]		
	^{10}B(p,p')^{10}B*	Ca	21	19	
		C	31[a]		27_{-4}^{+5}
^{10}B*(1.74)	^{9}Be(^{3}He,d)^{10}B*	Several	<0.3[b]		
		Au		<0.3	<0.3

[a] Reanalysis of data reported in Ref. 3.
[b] From Ref. 3.

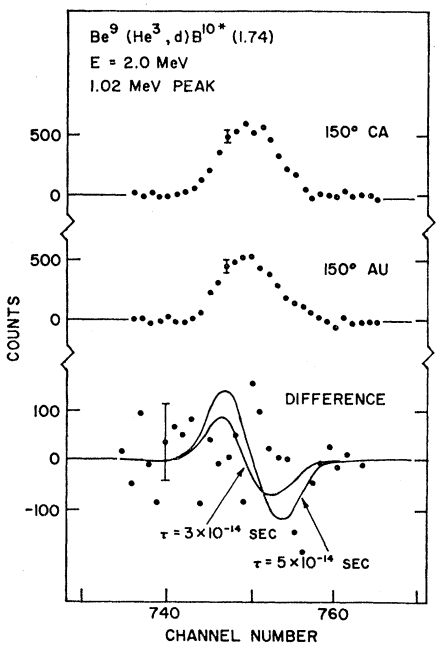

FIG. 10. Spectra at the backward angle for the 1.02-MeV γ ray from the reaction ^{9}Be(^{3}He,d)^{10}B*(1.74). The difference spectrum is obtained by subtracting the Au run from the Ca run. The curves are computer calculations for the indicated lifetimes.

The final values of the lifetimes are compared with those from other laboratories in Table VII. In general, the somewhat more precise values of the present work are in good agreement with the other results. In addition, it should be noted that the present results are self-consistent in that in several cases two lifetimes were measured in a single experiment and analyzed in identical fashion and interlocking values of the lifetimes were obtained.

VII. DISCUSSION

The lifetimes listed in Tables VI or VII, when combined with the appropriate branching ratios and quadrupole-dipole mixing ratios,[18] provide a set of transition matrix elements for comparison with theory, e.g., the effective-force shell-model calculations of Cohen and Kurath.[2] Moreover, a comparison of the lifetimes for the 2^+, $T=1$ multiplet tests more general,

TABLE VII. Comparison of lifetime results with those from other laboratories. All values are in units of 10^{-13} sec.

Level	This work	Ref. 6	Ref. 5
^{10}B*(1.74)	<0.3	<0.4	
^{10}B*(2.15)	27_{-4}^{+5}	21_{-5}^{+8}	
^{10}B*(3.59)	1.50±0.15	1.7±0.7	1.20±0.43
^{10}Be*(3.37)	1.89±0.20		1.6 ±0.3
^{10}C*(3.36)	1.55±0.25		

[18] E. K. Warburton, J. W. Olness, S. D. Bloom, and A. R. Poletti, Phys. Rev. (to be published).

model-independent properties of the nuclear matrix elements. Since these aspects have been discussed before by us[4] or by others,[18] we restrict ourselves to a summary of the results.

Using the lifetime values presented here, Warburton *et al.*[18] made a detailed comparison of the transition probabilities of the bound states in ^{10}B with the computations of Cohen and Kurath.[2] Special emphasis was put on the states at 2.15 and 3.59 MeV for which these authors[18] had determined the $E2/M1$ mixing ratios, including their signs. The model calculations did not agree very well with the observed transition strengths and, more significantly, they failed to give the correct signs for three out of four mixing ratios. However, if the two neighboring states with $J^\pi=1^+$, $T=0$ at 0.72 and 2.15 MeV were allowed to mix with each other, and similarly the $J^\pi=2^+$, $T=0$ state at 3.59 MeV with the next higher such state (not yet identified with certainty), the correct signs and amplitudes for all observed mixing ratios could be obtained.[18] (It is a necessary condition for theory to yield the correct sign,[19] and failure to do so indicates that even reasonable agreement between calculated and experimental lifetimes may be fortuitous.) The mixed wave functions then also give remarkably good agreement with the observed $M1$ and $E2$ matrix elements. In Table VIII we compare the experimental total γ widths with the ones calculated from the pure wave functions of Cohen and Kurath[2] and from the mixed wave functions of Warburton *et al.*[18] Obviously the mixed wave functions give much better agreement with the observed lifetimes. The $E2$ components in the computed widths contain the usual effective charge, $\epsilon_n=\epsilon_p=0.5$, and the radial integral is taken as $\langle\rho^2\rangle=7.056$ F^2.

The lifetime of the $J^\pi=0^+$, $T=1$ state at 1.74 MeV is in a sense quite insensitive to the model since the spin part of the $M1$ matrix element is fixed directly by the strength of the analog, allowed Gamow-Teller β decay from ^{10}C to the 0.72-MeV state in ^{10}B. The value of $ft=1.0\times10^3$ leads to a Γ_γ of 110 meV, which must then be modified to include the contribution of the space part of the matrix element.[20] The shell-model calculation gives 140 meV, while the mixed wave functions of Warburton *et al.*[18] yield 180 meV; both values are well above the observed lower limit of 22 meV. Whereas the mixing of the wave functions of the two neighboring 1^+, $T=0$ states leads to a cancellation in the calculation of the lifetime of the 2.15-MeV state, thus lengthening it considerably, the mixing affects the lifetime of the 1.74-MeV state only slightly. The wave function of the $J^\pi=0^+$, $T=1$ state at 1.74 MeV is assumed to be pure since the next such state is at least 5 MeV away.

TABLE VIII. Comparison of the radiative widths of low-lying levels in the mass-10 nuclei with the effective-force calculations of Cohen and Kurtha, and with the mixed wave function calculations of Warburton *et al.* which give the correct signs and magnitudes for $\delta=M(E2)/M(M1)$.

Level	Final levels (MeV)	$\langle\Gamma_\gamma$(meV)$\rangle$ Expt.	Theoret.[a]	Theoret.[b]
^{10}B(1.74)	0.72	>22	140	180
^{10}B(2.15)	1.74, 0.72, 0	0.244±0.041	1.445	0.114[c]
^{10}B(3.59)	2.15, 0.72, 0	4.39 ±0.44	7.076	5.45
^{10}C(3.36)	0	4.25 ±0.69	2.09[d]	4.32[e]
^{10}B(5.17)	1.74	<12	2.28[d]	4.52[e]
^{10}Be(3.37)	0	3.48 ±0.37	2.47[d]	4.73[e]

[a] Effective-force calculation, Refs. 2 and 20.
[b] Modified effective-force calculation, Ref. 18 and text.
[c] This value results from a cancellation of terms and is thus very sensitive to the wave functions.
[d] No effective charge used, $\langle\rho^2\rangle=10$ F^2.
[e] Effective charge $\epsilon_p=\epsilon_n=0.5$, $\langle\rho^2\rangle=7.065$ F^2, and pure wave functions assumed.

The $E2$ transitions in ^{10}C and ^{10}Be have also been computed by Kurath[20] with the effective-force model. Using $\langle\rho^2\rangle=10$ F^2, he obtains the values included in Table VIII, which are about a factor of two below the experimental results. We have recalculated the widths using the effective-charge correction (discussed, for example, by Poletti *et al.*[19]) with an effective charge $\epsilon_p=\epsilon_n=0.5$. The isoscalar part of the matrix element (see below) is thus multiplied by $1+\epsilon_p+\epsilon_n=2$ and the isovector part by $1+\epsilon_p-\epsilon_n=1$. Since the isovector part in Kurath's calculation is very small, the effective charge increases all three analog transition strengths by a factor of almost four. The radial integral $\langle\rho^2\rangle$ was changed to 7.056 F^2, which is the generally accepted average value in the $1p$ shell.[18,21] The results, listed in the last column of Table VIII, are in good agreement with the observed widths.

These two transitions in ^{10}C and ^{10}Be are analog transitions and their matrix elements are related by $M=M_0+M_1T_z$, where M_0 and M_1 are the isospin scalar and vector matrix elements, respectively. This relation assumes identical radial wave functions for analog states. If all three transition strengths in the $T_z=\pm1,0$ nuclei are known, this rule based only on the validity of the concept of isospin can be tested. It should be noted the $E2$ transitions are the lowest multipole order for which such a test is feasible, since for dipole and $M2$ transitions the $T_z=0$ component is either forbidden or hindered by an isospin selection rule. A search for the analog $E2$ transition in ^{10}B, which connects the 5.16- and the 1.74-MeV states, gave a negative result with a limit of $\Gamma_\gamma<12$ meV.[4] This limit is about a factor of 4 above the value which would allow a test of the isospin relation given above.

An actual comparison of the experimental ^{10}C and ^{10}Be lifetimes suggests that the wave functions of the two states may not be identical, i.e., the ^{10}Be state may decay somewhat more slowly than its analog in ^{10}C while the reverse is expected from the calculations. The most likely cause for this discrepancy, if it exists, lies with the radial wave function. The lifetime of the ^{10}Be state can be obtained exactly with a value of $\langle\rho^2\rangle=6.06$ F^2 as compared to $\langle\rho^2\rangle=7.065$ F^2 for ^{10}C. The former

[19] A. R. Poletti, E. K. Warburton, and D. Kurath, Phys. Rev. 155, 1096 (1967).

[20] D. Kurath, Argonne National Laboratory Report No. ANL-7108 1965 (unpublished).

[21] D. H. Wilkinson, Nucl. Phys. 85, 114 (1966).

value is in excellent agreement with the value of $\langle\rho^2\rangle = 6.15\pm0.35$ F^2 suggested by Wilkinson[21] as the best value in the ground-state radial integral for ^{10}B. The fact that $\langle\rho^2\rangle$ is larger for ^{10}C is plausible, since the first excited state in ^{10}Be is bound by -3.4 MeV, while the analog state in ^{10}C is bound by only -0.54 MeV.

In summary, it may be said that the experimental techniques used in the present work can determine lifetime values with errors of approximately 10%, which are produced chiefly by uncertainties in the energy-loss functions. Nuclear theory at present is on the verge of taking advantage of this accuracy. The mixed wave functions of Warburton *et al.*,[18] although giving good agreement with an impressive amount of experimental detail in ^{10}B, still fail to produce the observed lifetimes within the experimental errors, and, as the authors observe, it is not immediately obvious how the mixing of the wave functions was to be predicted. It appears that the Doppler-shift attenuation method when used in a careful and consistent manner, even with the present imperfect knowledge of the slowing down of ions in matter, has sufficient precision to test severely the presently available nuclear models.

ACKNOWLEDGMENTS

We are very grateful to J. B. Thomas for substantial help in the measurements and analysis and for useful discussions. We also thank E. K. Warburton *et al.* for communicating their results to us prior to publication. We have profited from several useful discussions with D. Kurath and E. K. Warburton.

APPENDIX A: TIME DISTRIBUTION OF EXCITED RECOILS

In Eq. (1) the projected velocity v_p is a function of t. We measure $v_p(t)$ in units of $v_0=c/137$ (and for convenience drop the suffix on v_p). Integration of Eq. (1) yields

$$e^{-2t/\alpha}=\frac{K-K_e+2K_3v^2(t)}{K-K_e+2K_3v^2(0)}\,\frac{K+K_e-2K_3v^2(0)}{K+K_e-2K_3v^2(t)}, \quad (5)$$

where $K^2=K_e^2+4K_nK_3$ and $\alpha=Mv_0/K$. When both sides of Eq. (5) are raised to the $\alpha/2\tau$ power one obtains the distribution in time $N[v(t)]$ of recoil nuclei with the velocity $v(t)$ at the moment of decay.

Although for purpose of a computer analysis Eq. (5) is perfectly adequate, a small simplification can be obtained using the fact that in the present work $K_3/K_e\ll1$ and $K_n/K_e\leq1$ (see Table I). Then $K\cong K_e+2K_nK_3/K_e$ which, when inserted in Eq. (5), yields the form for $N[v(t)]$ which was actually used in the present analysis:

$$N[v(t)]=e^{-t(E',E)/\tau}$$
$$=\left[\frac{K_n+K_ev^2(t)}{K_n+K_ev^2(0)}\,\frac{K_e+K_nK_3/K_e-K_3v^2(0)}{K_e+K_nK_3/K_e-K_3v^2(t)}\right]^{\alpha/2\tau}. \quad (6)$$

The γ-ray energies E' and E are related to the velocities $v(0)$ and $v(t)$, respectively, through

$$E'=E_0\{1+[v(0)/c]\cos\theta_l\}, \quad (7a)$$

$$E=E_0\{1+[v(t)/c]\cos\theta_l\}, \quad (7b)$$

where θ_l is the angle of recoil in the laboratory measured from the direction of the detected γ ray.

Equations (6) [or more generally (5)] and (7) establish an implicit relation between E', E, and τ. A computer-implemented method for evaluating Eq. (4) of the text to obtain $N(E)dE$ is given in Appendix B.

APPENDIX B: METHOD OF FITTING THE LINE SHAPES

From Eq. (3) the energy span of the vacuum line (at $\theta=0°$) is $2E_0v_r/c$, which is divided into $2n$ intervals of width $\Delta E'$ such that $n\Delta E'=E_0v_r/c$. The vacuum line shape is then approximated by

$$P(E)dE=P_j\Delta E', \quad j=1\rightarrow2n$$

where the P_j's can be determined by fitting the vacuum line shape.

The energy span of the stopped line (for $v_r\leq v_{c.m.}$) is $E_0(v_{c.m.}/c+v_r/c)$, which is divided into $m+n$ intervals of width $\Delta E=\Delta E'$ such that $m\Delta E=E_{c.m.}/c$ and $n\Delta E=E_0v_r/c$, as before. The stopped line shape $N(E)dE$, given by Eq. (4), is then approximated by

$$N_i\Delta E=\sum_{j=1}^{m+n}P_j\Delta E'\{\exp[-t(E_j',E_{i+1})/\tau]-(1-\delta_{i0})\exp[-t(E_j',E_i)/\tau]\}. \quad (8)$$

The term $\exp[-t(E_j',E_i)/\tau]$ is obtained from Eqs. (5) and (6) by identifying $v(0)$ with v_j and $v(t)$ with v_i and obtaining E_j' and E_i from Eqs. (7). Equation (8) represents the number of γ counts recorded in the ith intervals. The range of i is from 0 to $m+n$, and the total range of j is from $m-n$ to $m+n$. At the equivalent backward angle, the spectrum is reflected about E_0. The modification of Eq. (8) which takes into account the finite thickness of the target in which the recoil nuclei are produced is quite straightforward.

The expression in Eq. (8), modified for finite target thicknesses, has been incorporated into a multiparameter search routine written for a PDP-7 computer.[15] The six parameters available in the search are E_0, τ, a scaling parameter for the peak area, and three background parameters. The other information required is calculated or obtained by fitting the vacuum line shape with a separate search routine. One such piece of required information is a suitable shape to represent the detector resolution function. For full-energy peaks, a pure Gaussian shape was adequate. For two-escape peaks it was necessary to include an exponential tail on the high-energy side to account for small-angle Compton scattering of the escaping annihilation radiation.